Environmental Science
Water Research & Technology

ROYAL SOCIETY OF CHEMISTRY

PAPER

View Article Online
View Journal | View Issue

Cite this: *Environ. Sci.: Water Res. Technol.*, 2022, **8**, 3138

Full-scale aerobic granular sludge for municipal wastewater treatment – granule formation, microbial succession, and process performance†

Jennifer Ekholm, *[a] Frank Persson, [a] Mark de Blois,[b] Oskar Modin, [a] Mario Pronk, [cd] Mark C. M. van Loosdrecht, [c] Carolina Suarez, [e] David J. I. Gustavsson [fg] and Britt-Marie Wilén [a]

Aerobic granular sludge (AGS) plants have gained growing interest and application due to their low energy demand, small footprint, and low operational costs. However, the fulfilment of strict discharge limits for nitrogen and phosphorus, vast seasonal temperature variations, and large peaks in influent flows may pose challenges to the implementation of AGS. Moreover, the knowledge about microbial community assembly and process performance under varying environmental conditions in full-scale reactors is still limited. In this study, the first implementation of the AGS process in the Nordic countries was assessed. In two full-scale AGS reactors with different seeding sludges, the start-up was associated with rapid changes in microbial community composition in both, but only successful granulation in one. As a consequence, the non-granulated reactor was eventually reseeded with biomass from the better granulated reactor. This resulted in a convergence of the microbial communities in the two reactors with the maintenance of stable sludge concentrations (6–8 g L^{-1}) with large granules (50–80% with diameter >2 mm) and fast settling of biomass (SVI_{30}/SVI_{10} of 0.9–1). Immigration from the influent wastewater was a minor factor affecting the microbial community once the granules had formed, while the seasonal variations in environmental factors were identified as important. Key guilds of AOB (*Nitrosomonas*), NOB (mainly *Ca.* Nitrotoga), PAOs (mainly *Tetrasphaera*), and GAOs (mainly *Ca.* Competibacter) varied considerably in abundance throughout the study period. After 15 months, stable organic matter, nitrogen, and phosphorus removal were attained with low effluent concentrations. During the start-up, the BOD_7/N ratio, influent flow, and temperature were important factors influencing the performance of the AGS.

Received 22nd August 2022,
Accepted 4th November 2022

DOI: 10.1039/d2ew00653g

rsc.li/es-water

Water impact

The aerobic granular sludge (AGS) technology allows for simultaneous removal of nitrogen, carbon, and phosphorus, as well as fast settling, all in one reactor, which reduces energy demand and footprint. Little is yet known about AGS in full-scale, and no start-up studies have been made in countries with low temperatures. This study increases the knowledge about the microbial community assembly in AGS, its start-up and operation at varying temperatures.

1. Introduction

Aerobic granular sludge (AGS) is a biofilm process without the need for carrier material that has proved to hold several advantages in municipal wastewater treatment such as simultaneous removal of carbon, nitrogen and phosphorus, fast settling, small footprint, and low energy usage.[1,2] For example, full-scale AGS plants have been reported to have 25–75% reduced footprints and 20–50% reduced energy usage compared to similarly loaded conventional activated sludge (CAS) plants.[2,3] Resource recovery from the AGS process is promising, including energy, biopolymers and struvite.[4] AGS reactors are operated as sequencing batch reactors (SBRs)

[a] *Department of Architecture and Civil Engineering, Chalmers University of Technology, Sven Hultins gata 6, 412 96 Gothenburg, Sweden. E-mail: jennifer.ekholm@chalmers.se*
[b] *H2OLAND, Östra Vattugränd 2, 441 30 Alingsås, Sweden*
[c] *Department of Biotechnology, Delft University of Technology, Van der Maasweg 9, 2629 HZ Delft, The Netherlands*
[d] *Royal HaskoningDHV, Laan 1914 35, 3800 AL Amersfoort, The Netherlands*
[e] *Division of Water Resources Engineering, Faculty of Engineering LTH, Lund University, John Ericssons väg 1, 221 00 Lund, Sweden*
[f] *VA SYD, P.O. Box 191, 201 21 Malmö, Sweden*
[g] *Sweden Water Research, Scheelevägen 15, 223 70 Lund, Sweden*
† Electronic supplementary information (ESI) available. See DOI: https://doi.org/10.1039/d2ew00653g

with simultaneous plug-flow upward anaerobic feeding and effluent withdrawal, followed by an aerobic mixed reaction phase and settling.[5] Today, more than 80 AGS plants treating mainly municipal wastewater are operated around the world under the tradename Nereda®.[6] Operational results have been reported from a few of these full-scale reactors, located in Poland, the Netherlands, and South Africa.[3,5,7–9] These reactors generally show well-functioning removal of organic matter, nitrogen and phosphorus under their local conditions with, *e.g.*, large temperature variations.

The start-up of AGS reactors is expected to be slower than the corresponding CAS processes. The establishment of CAS with biological phosphorus removal can take just a few weeks,[10] while the start-up of full-scale AGS takes a considerably longer time.[5,11] AGS reactors that are completely seeded with AGS biomass can achieve biological nutrient removal within a few weeks. During start-up, the granules form, which is governed by selective settling and proliferation of slow-growing microorganisms in the bottom-fed reactors.[12,13] Modelling of AGS has shown that selective sludge wasting and selective feeding were the dominating drivers for the granulation rate.[11] However, the process is intricate and the factors affecting granule size and microbial composition are poorly understood.[14–16] A large number of studies on the microbial community structure and function in AGS have been conducted in lab-scale reactors receiving synthetic wastewater.[17] The formation of granules during the start-up of such reactors is generally associated with large changes in community structure.[18–23]

It is yet unknown how the microbial communities assemble during granule formation and steady-state operation in full-scale reactors. In full-scale, several important factors differ from the more investigated lab-scale reactors. The feed composition of real wastewater, in terms of the particulate and non-diffusible fractions of the organic matter, influences the structure of the granules since the microorganisms need to hydrolyse it to readily biodegradable COD before it can be assimilated, which favours fast-growing heterotrophic bacteria.[9] Layer *et al.* found that the particulate organic substrate promotes floc formation, smaller granules, and slower settling properties.[24] Hydrolysis of influent wastewater might be beneficial for AGS, as it is considered the rate-limiting step of conversion of substrates and increases the bioavailability of the organic matter.[25]

The temperature variation is another such factor. From studies on activated sludge, it has been shown that seasonal temperature variation has a major impact on microbial community dynamics.[26,27] The temperature was found to be one of the main drivers of community assembly in activated sludge, with the hypothesis that low solids retention time (SRT) in combination with low temperature may result in a reduction of slow-growing microbes and therefore contribute to seasonal shifts in the community.[26] Whether this is valid also for AGS with its biofilm growth mode is unknown.

A third factor typical for full-scale reactors is the immigration of microorganisms from the influent wastewater. In activated sludge, it has recently been demonstrated that the microbial community is strongly controlled by immigration.[28] In full-scale AGS, Ali *et al.* showed that the impact of immigration was larger on the microbial community in the flocs than the granules.[29] This suggests that immigration and species sorting (environmental and operational factors) affect flocs and granules to varying extent. Hence, the importance of immigration may even change in AGS during start-up when the granules form from activated sludge flocs.

In the municipality of Strömstad in Sweden, an AGS Nereda® plant was taken into commission at the Österröd wastewater treatment plant (WWTP) in June 2018. The location entails large seasonal variations in temperature, wastewater flow, and loads of organic matter and nutrients. In this study, we aim to identify patterns in the microbial community succession underpinning the formation and maintenance of AGS during the start-up of full-scale reactors. We furthermore assess the function of the reactors at the large seasonal variations.

2. Materials and methods

2.1. Description of the plant

The Österröd WWTP, Strömstad, Sweden (58°55′59.1″N 11°11′48.8″E), was upgraded in 2017–2018 with an AGS plant and primary settlers. After the upgrade, the existing CAS process was renovated and extended to be operated in parallel with the AGS plant. The capacity of the rebuilt WWTP is 30 000 population equivalents (P.E.) during the summer high season and 15 000 P.E. during the rest of the year. The design flow is 600 m^3 h^{-1} to the AGS and CAS, together. The AGS process, consisting of two AGS reactors, was designed to treat 60% of the flow, with the CAS treating the remaining 40%. However, the AGS plant treated 100% of the flow when the CAS reactor was renovated (October 2018 to June 2019). The influent wastewater comes from a combined sewer system resulting in increased inflow at rain events and sometimes also due to seawater intrusion. There is also a large increase in the organic- and nutrient load in the summer due to tourism. At this location, the period from June to August is considered summer, September to mid-November is autumn, then follows winter until mid-March and April–May is the spring. The targeted effluent concentrations (annual averages) from the AGS reactors were 8 mg L^{-1} of BOD_7, 10 mg L^{-1} of total nitrogen (TN), 1.0 mg L^{-1} of total phosphorus (TP), and 20 mg L^{-1} of suspended solids (SS).

The influent wastewater enters inlet screens, an aerated fat- and sand trap, primary settlers, biological treatment with AGS (with associated influent and effluent buffer tanks) in parallel with CAS (including a secondary settler), a flocculation tank for the effluents of the AGS and CAS (dosage of poly-aluminium chloride as precipitation chemical), and a final settler (Fig. 1). A flocculation tank is located prior to the pre-settlers (Fig. 1). The pre-settlers consist of three parallel tanks; one feeding only the AGS, one

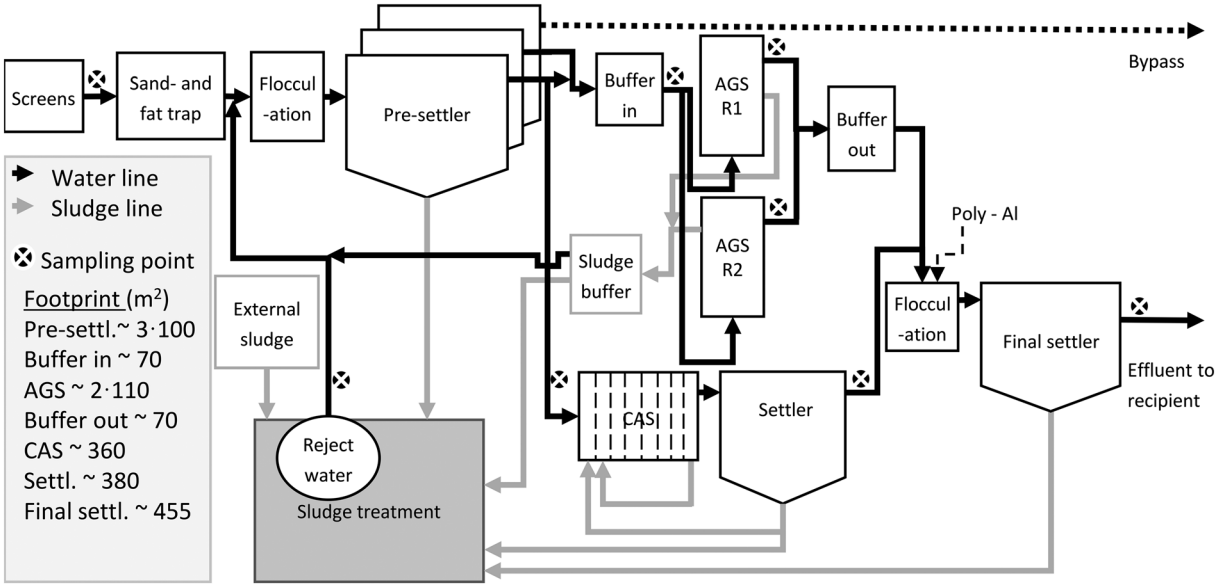

Fig. 1 Simplified process scheme (not in scale) of the Österröd WWTP.

feeding both the AGS and the CAS, and one solely used at peak flows to prevent overflow. The pre-settlers were designed for COD removal of 30%, based on expected loads, but the actual COD removal was higher (40–50%). The sludge treatment consists of storage tanks (partly aerated), a mechanical sludge thickener, and a sludge screw press. The reject water is pumped to the water line prior to the primary settler. Septic sludge is sent to the sludge line.

2.2. The AGS reactors

Each AGS reactor (R1 and R2) has a volume of 758 m^3 and a depth of 7 m. The influent and effluent buffer tanks have volumes of 340 m^3 and 440 m^3, respectively, and the buffer tank for discharged sludge has a volume of 30 m^3. The reactors are equipped with sensors for temperature, oxidation–reduction potential (ORP), dissolved oxygen (DO), and nitrate. The reactors also have analysers taking samples every ten minutes for measurement of ammonium and phosphate concentrations (Endress Hauser). The water level is tracked with an ultrasound sensor.

2.3. Sampling of water and sludge

Flow proportional water samples were collected from the influent and effluent of R1 and R2. The flow proportional sampling was out of operation in 2019 from April 1st to May 13th for the influent and from April 1st to July 22nd for the effluent. At those occasions, grab samples were taken. The sampling of sludge was done at the depths of 1.5 and 5 m with a Ruttner sampler during the aerated reactor phase. The samples from the two depths were mixed prior to analysis.

2.4. Influent wastewater characteristics

The composition of the influent wastewater, from July 2018 to September 2019, is shown in Table 1. The concentrations of organic matter, phosphorus and ammonium were higher in late spring and summer than in fall, winter, and early spring (Table 1), which can be explained by summer tourism and less rain in spring and summer. The concentration of easily degradable organic matter (BOD_7, soluble COD) in the AGS plant was considered low. To increase it, and thereby increase the BOD_7/N-ratio to the design value (>3), hydrolysis–fermentation was introduced in the pre-settler tank by increasing the sludge level from August 31st, 2019 (Table 1).

2.5. Seed sludge and reactor operation

AGS R1 was seeded with activated sludge from a neighbouring WWTP (Bodalen WWTP in the municipality of Tanum, average load 3000 P.E.), an SBR plant with compact and well-settling sludge (average SVI_{30} of 67 mL g^{-1} in January to May 2018). AGS R2 was seeded with granules from the AGS at the Simpelveld WWTP in the Netherlands (average load 9000 P.E.).[6] Both seeding sludges treated municipal wastewater with enhanced biological nitrogen- and phosphorus removal. The seeding was performed in June 2018 to a sludge concentration of 3.4 and 3.6 g L^{-1} for R1 and R2, respectively. Due to the low sludge concentration in March 2019 (about 2.5 g L^{-1}) and lack of nitrification, R1 was reseeded with granules from R2. The temperature was at its highest (about 20 °C) when the seeding was done, whereafter the temperature decreased to 6 °C during the following six months (Fig. 2).

A cycle in the AGS reactors starts with a fixed time for simultaneous filling of influent wastewater and decanting of effluent followed by sludge discharge. Then follows a reaction phase consisting of a main aeration phase and sometimes a pre-and/or post-denitrification phase. The cycle is terminated by a settling phase with a fixed time. In the post-

Table 1 Composition of pre-settled wastewater feeding the AGS reactors, average ± standard deviation (*n*), where n is the number of samples

Period	Concentration (mg L^{-1})									Ratio	
	BOD_7	COD	Soluble COD	TP	TN	TKN	NH_4^+-N	NO_3^--N	SS	BOD_7/TKN	BOD_7/TP	Soluble COD/COD
Jul–Sep 2018	141 ± 74 (16)	312 ± 127 (34)	170 ± 88 (34)	5 ± 2 (34)	48 ± 17 (14)	47 ± 17 (15)	41 ± 17 (34)	0.8 ± 0.7 (18)	78 ± 33 (16)	3.1 ± 1.2 (8)	28.7 ± 11.1 (8)	0.57 ± 0.12 (22)
Oct–Dec 2018	61 ± 20 (24)	163 ± 65 (36)	86 ± 58 (36)	3 ± 1 (37)	41 ± 6 (9)	31 ± 10 (23)	24 ± 8 (39)	2 ± 1 (15)	69 ± 26 (24)	2.3 ± 0.94 (12)	16.4 ± 7.8 (14)	0.54 ± 0.16 (23)
Jan–Mar 2019	54 ± 29 (24)	131 ± 59 (24)	64 ± 21 (24)	3 ± 1 (24)	0	29 ± 12 (24)	23 ± 10 (24)	0	59 ± 29 (24)	1.8 ± 0.54 (12)	20.3 ± 6.0 (12)	0.52 ± 0.083 (12)
Apr–Jun 2019	97 ± 34 (24)	238 ± 64 (24)	107 ± 24 (24)	5 ± 1 (24)	49 ± 7 (12)	48 ± 8 (24)	40 ± 6 (24)	38 ± 14 (18)	78 ± 26 (24)	2 ± 0.64 (12)	19.6 ± 5.32 (12)	0.46 ± 0.063 (12)
Jul–Sep 2019	124 ± 44 (14)	261 ± 56 (14)	117 ± 30 (14)	5 ± 2 (14)	53 ± 19 (14)	52 ± 19 (14)	41 ± 14 (14)	0.1 ± 0.02 (14)	78 ± 30 (14)	2.5 ± 0.66 (14)	27.0 ± 3.9 (14)	0.45 ± 0.071 (14)
Oct 2019	115 ± 48 (4)	230 ± 106 (4)	86 ± 21 (4)	3 ± 1 (4)	23 ± 12 (4)	23 ± 12 (4)	18 ± 9 (4)	0.1 ± 0 (4)	99 ± 21 (4)	5.2 ± 0.49 (4)	45.4 ± 6.6 (4)	0.42 ± 0.15 (4)

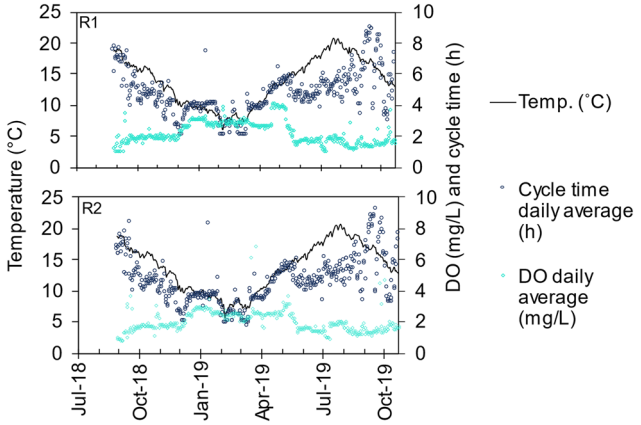

Fig. 2 Temperature, daily average cycle time and daily average DO concentration for R1 and R2.

denitrification phase, aeration in short pulses was applied to mix the reactor content, since no mixers are installed in Nereda reactors. With a fixed filling time, the exchange ratio is dictated by the inflow. Typical exchange ratios were 35–50% (Table 2). The total cycle time was decided by a model (Aquasuite® Nereda controller) based on the predicted inflow. The total cycle time, and as result, the hydraulic retention time (HRT), were hence, shorter during wet weather flow than during dry weather flow (Table S1†). The time of the aerated phase is determined by the control system with input from the online measurement of ammonium (the aeration phase ended when 3–3.5 mg L^{-1} was reached). The DO concentration was controlled by a set-point, typically set at a higher value during the colder months (2.5–3 mg L^{-1}) than during the warmer months (1–2 mg L^{-1}) to maintain nitrification (Table 2).[30]

During the first three months, the strategy was to gradually increase the up-flow velocity during filling and decanting to promote fast-settling aggregates but avoid excessive wash out of biomass. This strategy was followed in R2, but not in R1, where the up-flow velocity had to be decreased after six months when the biomass concentration was critically low. After the reseeding in March 2019, the up-flow velocity could eventually be increased also in R1 (Table 2).

2.6. Reactor loads

The specific loads of BOD_7, total Kjeldahl nitrogen (TKN) and TP were higher in R1 than R2 prior to the reseeding, whereafter the loads became more similar (Fig. S1†). From April 2019 onward, the specific loads of TKN and TP decreased for both reactors, and the load of BOD_7 remained around 0.03 kg (kg VSS^{-1} d^{-1}). Over the whole study period, the average specific COD loads were 0.12 and 0.084 kg COD (kg VSS^{-1} d^{-1}) for R1 and R2, respectively, and the average volumetric loads of COD were 0.41 and 0.43 (kg COD m^{-3} d^{-1}). The mass load (kg d^{-1}) of BOD_7 and SS was generally

Table 2 Operational parameters of the AGS reactors, average ± standard deviation, *n* is the number of samples

R1	Temp (°C)	Flow (m^3 d^{-1})	DO (mg L^{-1})	Cycle time (h)	HRT (h)	Upflow velocity (m h^{-1})	Exchange ratio	*n*
Jul–Sep 2018	17.4 ± 1.1	1190 ± 429	1.7 ± 0.5	6.2 ± 1.0	14.4 ± 5.2	3.1 ± 0.3	0.43 ± 0.04	34
Oct–Dec 2018[a]	12.8 ± 2.3	1975 ± 459	2.1 ± 0.4	4 ± 0.9	9.6 ± 1.9	3.1 ± 0.4	0.40 ± 0.06	92
Jan–Mar 2019[a]	8.4 ± 0.9	2069 ± 611	2.9 ± 0.2	2.6 ± 0.9	10.2 ± 2.9	2.3 ± 0.4	0.31 ± 0.06	90
Apr–Jun 2019[a]	13.9 ± 2.2	1441 ± 247	2.5 ± 0.9	4.7 ± 0.6	12.3 ± 2.2	3.1 ± 0.4	0.38 ± 0.08	88
Jul–Sep 2019	18.4 ± 1.2	1362 ± 320	1.5 ± 0.3	5.6 ± 0.3	15.2 ± 4.3	3.4 ± 0.0	0.37 ± 0.07	92
Oct 2019	14.2 ± 1.0	1389 ± 542	1.7 ± 0.4	5.7 ± 0.8	13.7 ± 4.9	3.4 ± 0.0	0.43 ± 0.07	30
R2								
Jul–Sep 2018	17.4 ± 1.1	1189 ± 448	1.5 ± 0.7	6.2 ± 1.1	14.9 ± 8.2	3.1 ± 0.6	0.43 ± 0.04	34
Oct–Dec 2018[a]	12.8 ± 2.3	2144 ± 664	2.0 ± 0.4	3.9 ± 0.8	9.3 ± 2.3	3.4 ± 0.0	0.42 ± 0.08	92
Jan–Mar 2019[a]	8.4 ± 0.9	2595 ± 959	2.6 ± 0.6	3.1 ± 0.9	9.1 ± 3.7	3.4 ± 0.2	0.38 ± 0.09	90
Apr–Jun 2019[a]	13.9 ± 2.2	1521 ± 287	2.1 ± 0.6	4.6 ± 0.7	12.5 ± 3.1	3.4 ± 0.2	0.38 ± 0.10	88
Jul–Sep 2019	18.4 ± 1.2	1333 ± 313	1.5 ± 0.3	5.6 ± 1.3	15.1 ± 3.7	3.4 ± 0.0	0.37 ± 0.08	92
Oct 2019	14.2 ± 1.0	1500 ± 575	1.9 ± 0.8	5.7 ± 1.7	13.2 ± 4.5	3.4 ± 0.1	0.43 ± 0.07	30

[a] Period when the CAS was out of operation.

lower than the design values (Fig. S2, Table S2†), while for TKN and TP it was often higher (Fig. S2, Table S2†).

2.7. Technical challenges

One main challenge during the start-up was the disconnection of the CAS plant from October 2018 to July 2019. This resulted in flow- and mass load exceeding the designed values of the AGS plant. A leaking valve also resulted in a loss of sludge from R1, probably from the early start-up until August 21st, 2019. See the ESI† for a summary of technical start-up experiences.

2.8. Analyses of water and sludge

Analyses of BOD_7, COD, ammonium, nitrate, nitrite, TKN, TN, phosphate and TP were performed on influent and effluent samples according to standard methods.[31] Soluble COD was determined after filtration through 0.45 μm pore size filters.

The sludge properties were measured according to standard methods with analyses of mixed liquor suspended solids (MLSS), volatile suspended solids (VSS), total solids (TS), volatile solids (VS) and sludge volume index (SVI) after 10 and 30 minutes.[31] The size distribution of the sludge and granules was determined by sieving one litre of sludge through a series of sieves with pore sizes of 2, 1.4, 0.6, 0.4 and 0.2 mm. The washed sample remaining on each sieve was dried at 105 °C. The fraction <0.2 mm was calculated by subtracting the sum of the sieved samples from the TS. The sludge samples were examined monthly by light microscopy (Olympus BX53) with micrographs taken by a digital camera (Olympus DP11).

2.9. Microbial community analysis

2.9.1. DNA extraction, PCR, amplicon sequencing, and data analysis. A total of 24 samples of biomass from each reactor, six grab samples of influent- and 12 samples of effluent biomass were investigated by amplicon sequencing. Reactor biomass was collected by centrifugation (3000 × *g*, 5 min) of 15 mL sludge, while influent and effluent biomass was collected on sterile membranes (0.2 μm, Sartorius Stedim Biotech). Sludge pellets and membranes were stored at −20 °C. Prior to DNA extraction, thawed sludge pellets were homogenised using a BagMixer 100 Minimix (Interscience) for six minutes. DNA was extracted from 350 μL of homogenised sludge and membranes using the FastDNA spin kit for soil (MP Biomedicals).

The V4 region of the 16S rRNA gene was amplified by PCR using the primers 515′F and 806R, to cover both bacteria and archaea.[32,33] Sequencing was conducted on a MiSeq (2 × 300) using reagent kit V3 (Illumina) resulting in 89 649 to 688 416 sequence reads per sample. See the ESI† (supplementary details on amplicon sequencing) for details on DNA extraction, PCR, purification, quality control and sequencing. Sequence processing and generation of count tables with amplicon sequence variants (ASVs) were carried out using two independent pipelines; DADA2 v.1.16 (ref. 34) and VSEARCH v.2.13.1.[35] A consensus count table of ASVs from the two pipelines was generated in qdiv.[36] The count table was rarefied to the lowest number of reads (65 984) using subsampling without replacement. Taxonomy was assigned with SINTAX[37] within VSEARCH using the Silva database v.132.[38] Data visualisation and multivariate statistics were conducted in qdiv, as well as the packages vegan[39] and phyloseq[40] in R (**https://www.r-project.org/**). Raw sequence reads are deposited at the NCBI sequence read archives (SRA) accession PRJNA856974.

2.9.2. Fluorescence *in situ* hybridisation (FISH) and confocal microscopy. FISH on cryosections of granules was carried out as previously described.[20] Briefly, granules fixed in 4% paraformaldehyde (Gram-negative bacteria) or ethanol (Gram-positive bacteria) were embedded in O.C.T compound (VWR) and sliced in 20 μm cryosections. FISH was conducted with FAM-, Cy3- and Cy5-labelled probes (Eurofins Genomics,

Germany) (Table S3†) and SYTO40 counterstaining (ThermoFisher). DAPI (ThermoFisher) was used to simultaneously target poly-P granules, with emissions above 530 nm targeting poly-P.[41] Slides were mounted with Prolong Glass Antifade Mountant (ThermoFisher). Confocal microscopy was carried out using a Zeiss LSM700 (Carl Zeiss, Germany) with a 40×/1.3 apochromatic objective using 405, 488, 555 and 639 nm laser lines in frame mode with averaging = 4 and pinhole size equivalent to 1 AU at 639 nm. Large pictures were acquired with the tile function of the ZEN software and were reconstructed with Fiji[42] using the Grid/Collection Stitching plugin.[43]

3. Results

3.1. Sludge characteristics

In R1, which was seeded with activated sludge, small and irregularly shaped granules with finger-like outgrowths were observed already in August 2018 and remained like that during autumn and winter, whereas in R2, seeded with granular sludge, large, compact and mostly spherical granules were observed throughout the start-up period (Fig. S3†). The sludge volume index (SVI_{30}) remained higher for R1 (around 70–150 mL g^{-1}) than R2 (around 50–80 mL g^{-1}) during the start-up (Fig. 3B). The sludge concentration in R2 increased to around 8 g L^{-1} during the first five months of operation whereas, in R1, the sludge concentration remained at 2–3 g L^{-1} (Fig. 3A). Reseeding with granular sludge from R2 (well-mixed reactor content, 8 g L^{-1}) to R1 was carried out in March 2019 to improve sludge characteristics and reactor performance. This resulted in an increase in the sludge concentration from 2.5 g L^{-1} to 4 g L^{-1} in R1, whereas it decreased in R2 from around 8 to 6 g L^{-1} (Fig. 3A). From April 2019 both reactors had stable values of SVI_{30} (approximately 50 mL g^{-1}) and the ratio between SVI_{30} and SVI_{10} was generally close to 1, indicating quick settling of well-granulated sludge (Fig. S4†).

The biomass size distribution developed differently in R1 and R2 (Fig. 3D and E). In R2, the biomass aggregates gradually increased in size, with granules >2 mm dominating after eight months of operation. Also in R1, the biomass aggregates increased in size during the first months, but the process was slow and larger granules (>1.4 mm) were few until after reseeding. From May 2019 onward, granules exceeding 2 mm dominated also in R1. The percentage of the biomass consisting of flocs (<0.2 mm) fluctuated for both reactors and was 40 ± 20% and 21 ± 17% for R1 and R2, respectively. In R1, the floc fraction decreased to the level in R2 after the reseeding.

The concentration of suspended solids in the effluent was generally below 20 mg L^{-1} (Fig. 3C). The suspended solids in the effluent represent the fraction of the biomass with a lower settling velocity than the feeding up-flow velocity of 2.3–3.4 m h^{-1} (Table 2).

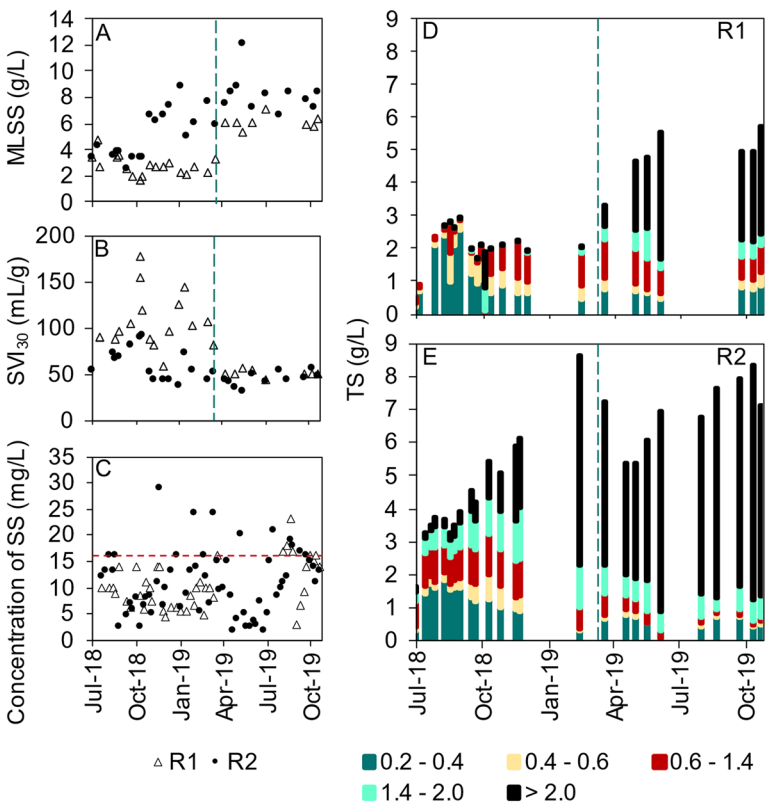

Fig. 3 A) The concentration of MLSS and B) SVI_{30} for R1 and R2. The dashed line marks the reseeding of R1. C) The concentration of suspended solids in the effluent, horizontal dashed line marks the effluent limit of 20 mg SS per L. The size distribution of the biomass (TS) in R1 (D) and R2 (E).

3.2. Microbial community diversity and succession

The microbial community of the biomass in the reactors (both floccular and granular sludge), the pre-settled influent and the effluent of the AGS was investigated by amplicon sequencing, covering the study period of 490 days. Diversity was measured as Hill numbers with diversity order q.[44] At q = 0, all amplicon sequence variants (ASVs) are given equal weight irrespective of their relative abundances and the alpha diversity is identical to the richness, *i.e.*, the number of ASVs detected in a sample. At q = 1, the relative abundances of ASVs are taken into account, and the diversity can be interpreted as the number of "common" ASVs. The Hill number framework was also used to measure dissimilarity (^{q}d) between communities.[45]

The diversity within samples (alpha diversity) was similar in both reactors with an observed richness (q = 0) in the order of 1000 ASVs (Fig. 4A). Alpha diversity varied more pronouncedly at q = 0 than q = 1 with a slight increase in diversity at the end of the study period (q = 0). Furthermore, the microbial communities in the reactors were more diverse than the influent (higher community richness) (p < 0.05) and effluent (p < 0.05) communities (Fig. S5†) for both q = 1 and q = 0, except for R1 compared to its effluent (q = 0, p = 0.06).

The microbial community composition was dynamic over time. The rate of change of the microbial communities, calculated as dissimilarity (q = 1) divided by the time elapsed between consecutive samples, decreased notably during the first months of operation, and R2 reached a stable rate of change more quickly than R1. Thereafter, the microbial communities in the two reactors changed at the same rate (Fig. S6†). With q = 0, similar but less clear patterns were observed (Fig. S6†).

The microbial communities in the two reactors clearly separated (x-axis) and changed over time (y-axis) as can be seen from the principal coordinate analysis (q = 1, Fig. 4B). R1 slightly converged with R2 already before the reseeding, and after the reseeding, the two reactors became highly similar.

The periodicity of the microbial community composition was assessed as dissimilarity (q = 1) as a function of the time gap between samples in R2, averaging over ten values in a moving window. The average dissimilarity increased up to a

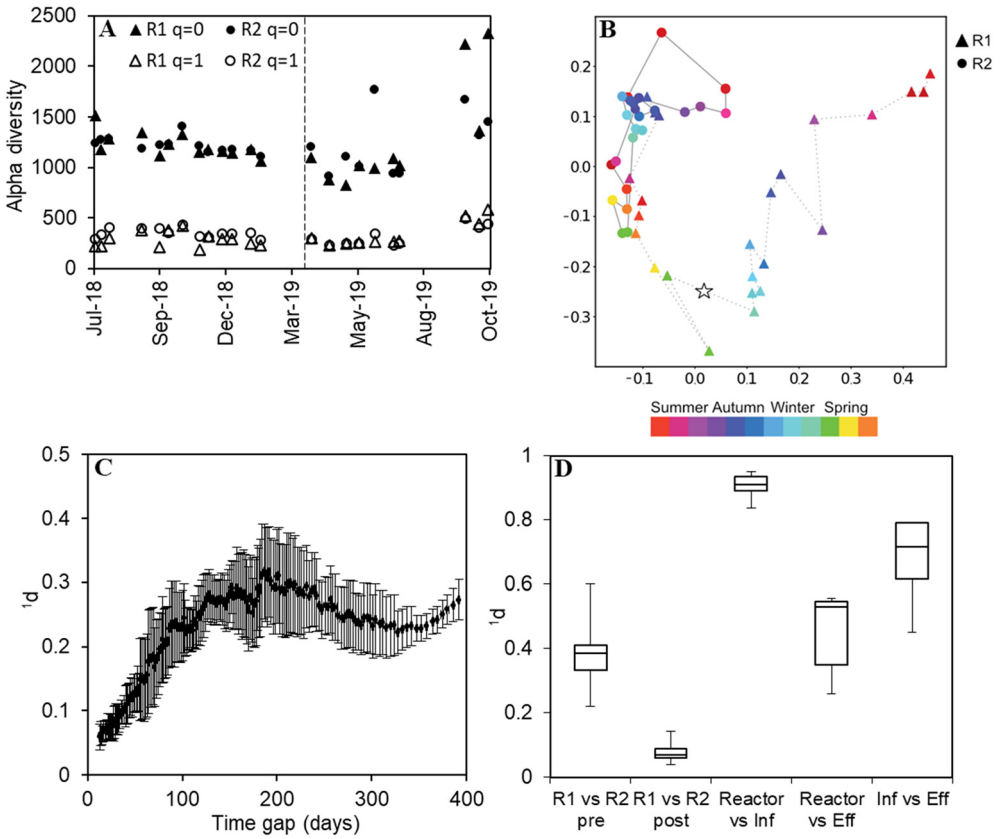

Fig. 4 A) Alpha diversity of the microbial communities in the biomass over time. The dashed line marks the reseeding. B) PCoA ordination (q = 1) of the biomass microbial communities in R1 and R2. The star marks the reseeding, x-axis PC1 (21.3%) and y-axis PC2 (17.2%). C) Dissimilarity (q = 1) as a function of the time gap between biomass microbial communities in R2. Each point represents a moving window average of 10 samples, error bars show the standard deviation. D) Boxplot of pairwise dissimilarities (q = 1). From left to right: dissimilarities between R1 *versus* R2 pre reseeding, R1 *versus* R2 post reseeding, reactors (R1 and R2) *versus* influent, reactors (R1 and R2) *versus* effluent, and influent *versus* effluent. In the boxplot, centre line: median, box limits: upper and lower quartiles, whiskers: minimum and maximum.

time gap of about 200 days and decreased again with a longer time gap until a new minimum was reached after about 350 days (Fig. 4C). This indicates that the communities were more similar after 350 days than after 200 days.

Pairwise dissimilarities (q = 1) between sample types highlighted the similar reactor community composition after reseeding (Fig. 4D). A somewhat lower similarity was observed with q = 0 (Fig. S7†), indicating that rare taxa contributed to the dissimilarity between the reactors. Compared with the microbial community in the influent, the reactor biomass was highly dissimilar (Fig. 4D). It was also evident that the effluent microbiome differed from the reactor biomass, although to a lesser extent (Fig. 4D).

The relative abundances of the main phylogenetic classes and the 20 most abundant genera in R1 and R2 are shown in Fig. S8 and S9.† No dramatic shifts were observed at the class level over time and between the reactors, while considerable dynamics were observed at the genus level. It was for instance demonstrated how some community members were washed out from the reactors quickly after start-up (*e.g.*, ASV5 and ASV56 within *Bacteroidota* and *Chloroflexi*, respectively) and how reseeding of R1 altered the abundance of *Tetrasphaera* and *Ca.* Competibacter (Fig. S8†) as well as *Trichococcus* and *Ca.* Microthrix (Fig. S10†).

Within the functional groups of putative polyphosphate-accumulating organisms (PAOs), glycogen-accumulating organisms (GAOs), ammonia-oxidizing bacteria (AOB), and nitrite-oxidizing bacteria (NOB), each genus harboured several ASVs. These ASVs had dynamic relative abundances over time in the reactor microbial communities (Fig. 5). Some of the ASVs showed similar dynamics within the same genus, for example within *Ca.* Nitrotoga and *Tetrasphaera*. The relative abundance of all ASVs within the functional groups of putative PAOs, GAOs, AOB and NOB also varied over time and between reactors (Fig. S11†). For instance, putative PAOs (*i.e.*, *Tetrasphaera*, *Dechloromonas*, *Ca.* Accumulibacter) and GAOs (*i.e.*, *Ca.* Competibacter, *Propionivibrio*) were especially low in R1 before the reseeding. As a result of the limited granulation and slow settling in R1 (Fig. 3B and D), the biomass would not be primarily located at the reactor bottom during anaerobic feeding where the exposure to easily available organic matter would be the highest, which likely

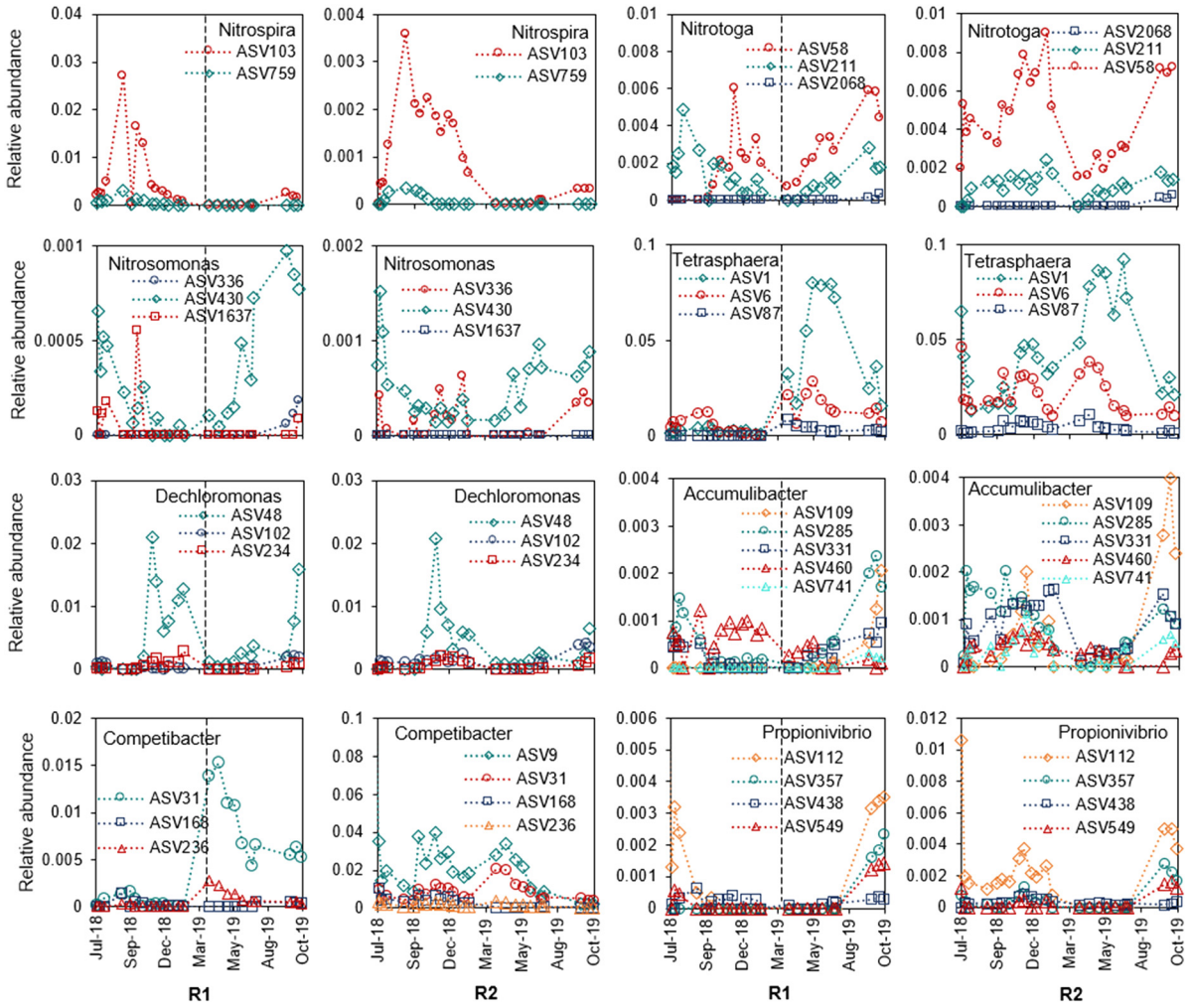

Fig. 5 Dynamics within genera (different ASVs of the same genus) in relative abundance over time in R1 and R2.

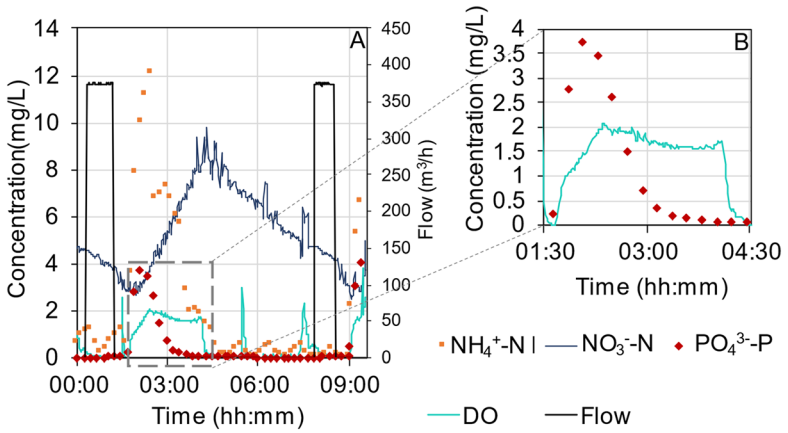

Fig. 6 A) Cycle concentrations of ammonium, phosphate (online analysers), nitrate and DO (online sensors) together with feed flow in R1, 13th of October 2019. B) Insert showing phosphate and DO concentrations at higher resolution.

prevented the growth of PAOs and GAOs. The highest relative abundance of putative PAOs in both reactors was found in the spring and summer of 2019. Although the functional groups varied in abundance over the year, there was no clear correlation with water temperature for any of the groups (Fig. S12 and S13†).

3.3. Localisation of functional groups in the granules

The localisation of different microbial groups in randomly selected granules was evaluated by FISH on cryosections of entire granules. AOB within *Nitrosomonas* and NOB within *Ca.* Nitrotoga tended to be located close to the surface with some colonies detected deeper inside the granule (Fig. S14A and B†). Filamentous bacteria within *Trichococcus* were detected in R1 (December 2018), throughout the entire small granule (Fig. S14C and D†). Likewise, putative PAOs within *Tetrasphaera* and *Ca.* Accumulibacter (Fig. S15†) were detected in the whole section of a mature granule (R2), whereas GAOs within *Ca.* Competibacter were mainly located in the inner granule parts. Of the PAOs, a positive signal for poly-P storage was observed for *Tetrasphaera* (Fig. S15E†). In addition, the innermost core of many of the larger granules had voids empty of cells, exemplified in Fig. S15C.†

3.4. Process performance at various operational conditions

The concentration profiles of ammonium, nitrate, phosphate and DO in R1 (October 2019) represent reactor performance when effluent compliances were met (Fig. 6A). First after that the aeration has started and the reactor content becomes mixed, will the concentration peaks appear in the online data. The concentrations of ammonium and phosphate were decreasing during the main aeration, while the concentration of nitrate increased as a result of the nitrification. Nitrate was partly removed in the aeration phase by simultaneous nitrification–denitrification (SND). In the following phase with pulse aeration, the nitrate decreased *via* denitrification. In this cycle, the phosphorus release was comparably small, and the aeration time was sufficient to reach close to 0 mg PO_4^{3-}-P per L (Fig. 6B). However, in previous periods (summer 2019), suboptimal removal was sometimes observed when the rates of phosphorus uptake slowed down before the end of the aeration phase and stopped at phosphate concentrations similar to in the influent (Fig. S16†). A large fraction of the soluble COD was taken up at the beginning of the cycle, as estimated by the concentration in the influent, samples taken five minutes into the aeration phase, and the effluent (Fig. S17†).

Average effluent concentrations from the AGS plant are summarized in Table S4.† The effluent BOD_7 was mainly particle-bound with fluctuating concentrations at an average of <8 mg L^{-1} (Fig. 7A). Total COD was removed to an average effluent concentration of 50.1 ± 21.1 mg L^{-1} (Table S4†). The nitrification worked relatively well when the CAS was in operation, but large fluctuations occurred when it was not and the AGS plant received the entire incoming flow causing short cycle times (Fig. 7B). The effluent concentrations of phosphate and TP varied considerably and were often high

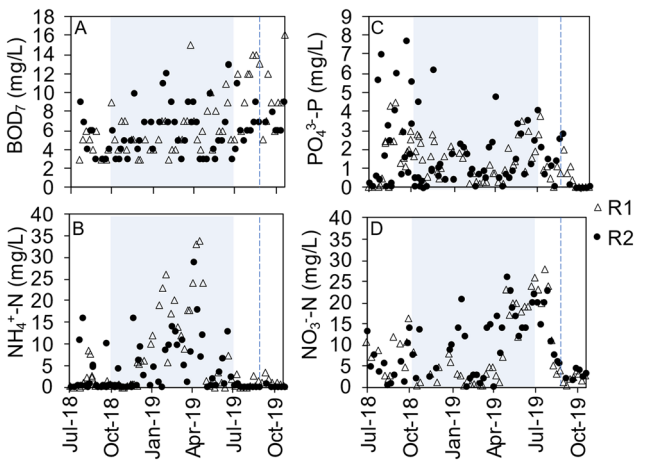

Fig. 7 Effluent concentration from R1 and R2. A) BOD_7, B) NH_4^+-N, C) PO_4^{3-}-P, and D) NO_3^--N. The shaded box represents the time when the CAS was taken out of operation. The dashed blue line marks the beginning of hydrolysis–fermentation in the pre-settler.

until October 2019 when phosphate concentrations were stable at around 0.03 mg P per L (Fig. 7C and S18†). Furthermore, incomplete denitrification resulted in periods with high nitrate concentrations in the effluent until October 2019 when effluent nitrate concentrations were stable below 5 mg N per L (Fig. 7D).

The specific nitrification rates were low for both reactors at the end of January and February 2019 and then increased during spring with a peak in the summer (Fig. S19†). R1 had higher specific nitrification rates than R2 at the beginning of the study; during this time the lower MLSS concentration in R1 was not limiting the performance (Fig. S19†). Over the entire study period, the applied loads of ammonium matched the conversion rates fairly well, except from November 2018 to April 2019 when the CAS was out of operation and the applied loads (above design capacity) exceeded the conversion rates (Fig. S20†). The nitrification rates in both reactors were the highest in the warmer months of the second summer (July and August 2019, Fig. S21†). The corresponding post-denitrification rates also peaked in this period, especially in R1 (Fig. S21†).

4. Discussion

The formation and maintenance of AGS in two full-scale reactors during seasonal fluctuations of nutrient concentrations, flow and temperature were investigated. The reactors were started up with different seeding sludges and the factors that shape the granules in terms of microbial community assembly, spatial organisation and functional performance were assessed and connected to treatment performance.

4.1. Granulation

R1 was seeded with activated sludge and R2 with aerobic granules, both types of inocula were taken from well-performing plants with biological removal of organic material, nitrogen, and phosphorus. In R1, granulation was slow and did not result in biomass with large and fast-settling granules, while granulation was maintained in R2 with a gradual increase in granule size (Fig. 3). R1 was reseeded with granules from R2, and the MLSS concentrations increased to similar concentrations as in R2 after a few weeks. At the same time, the SVI_{30} decreased to around 50 g mL^{-1} and the fraction of larger granules (>1.4 mm) increased. In R2, the granule/sludge bed settled below the sludge discharge outtake, creating a selection for dense granules early on. Although several environmental factors influence the granulation process,[46,47] the selective removal of the floccular fraction is key to granulation.[48] Since R1 contained large fractions of floccular sludge and small granules prior to reseeding, the sludge discharge resulted in incomplete removal of the floccular fraction as well as the removal of small granules, which occurred frequently (every cycle) due to the short cycle times. This in combination with the low sludge concentration and a leaking valve for sludge discharge resulted in a low SRT, which prevented growth of slow-growing microorganisms needed for the granulation.[12] The recurrent removal of small granules formed in R1 through the leaking valve, probably also contributed to the lack of increase in granule size. Furthermore, the lower up-flow velocity during the simultaneous filling and decanting in R1 (Table 2) likely allowed for more flocs to stay in the reactor. In addition, the low temperatures during winter slowed down the microbial growth rate and thereby worsened the conditions for granulation. Despite the troublesome start-up of R1, we believe that start-up of AGS from activated sludge would be possible under conditions similar to those at the Österröd WWTP, with careful operation using the experience of documented start-ups, like this one. Both surplus granular sludge and floccular activated sludge have been applied as seeding biomass in full-scale and pilot-scale studies applying real wastewater,[5,7,49] and lab-scale studies have shown that granules can form even at temperatures as low as 7 °C.[50] One important aspect that characterises the Österröd start-up and contributed to the problems with granulation from activated sludge (R1) was the lack of flexibility. When the CAS was out of operation, there was no possibility to adjust the flow, and there was also very little flexibility in the operation of the sludge discharge. When seeded with surplus sludge (almost without granules) from an existing AGS plant, the biomass concentration can reach 8–10 g L^{-1} after approximately nine months, but after a much shorter time (*ca.* three months) the flow- and treatment capacity can be reached.[5] At the Österröd AGS plant, the biomass concentration stabilized at 6–8 g L^{-1} (Fig. 3A).

Granules with irregular and sometimes filamentous outgrowths were frequent in both R1 and R2 (Fig. S3†). This granule morphology can be caused by high concentrations of particulate organic matter and may affect the settling properties.[24,51] Towards the end of the study period, most of the granules were large (>2 mm in diameter, Fig. 3D and E), but the reactors also contained fractions of floccular biomass (around 20%). Floccular biomass can originate from eroded granular fragments but also from suspended growth.[52,53] Probably, the complex organic matter in the influent was not entirely hydrolysed and consumed in the anaerobic phase, but also supported the growth of heterotrophic bacteria in the floccular and granular sludge during the subsequent aerobic phase. Several genera of heterotrophic bacteria were indeed detected in the biomass samples. In R1, filamentous *Trichococcus* (fermentative and able to denitrify) and *Ca.* Microthrix (consume long-chain fatty acids) were highly abundant with peaks during the winter and spring. *Terrimonas*, which is an aerobic heterotroph, was also abundant in both reactors throughout the study period.[54] The location of *Trichococcus*, evenly distributed in a small granule from R1, also suggests that organic carbon was available in the inner parts of the granules (Fig. S14C and D†). It was furthermore observed that in R1, *Trichococcus* and *Ca.* Microthrix decreased in abundance after reseeding with a concurrent increase in abundance of PAOs and GAOs (Fig.

S10†), improved SVI and formation of large granules (Fig. 3), supporting the importance of guilds capable of anaerobic storage of COD for the granulation.[12] In particular, PAOs will contribute to granule formation due to their mode of growth that forms dense, compact and fast-settling aggregates.[14] It has also previously been observed that the abundances of functional groups responsible for nitrogen and phosphorus removal were positively correlated with an increase in microbial aggregate size in full-scale AGS.[29]

4.2. Community succession and diversity

4.2.1. Alpha diversity was similar between the reactors and over time. Alpha diversity was similar in R1 and R2 with limited changes over time (Fig. 4A) despite the considerable differences in granulation with small sludge-like aggregates in R1 and considerably large granules in R2 in the first phase of the study period. Microbial biofilms, such as granules, are generally assumed to harbour highly diverse communities due to the many niches available.[55] However, activated sludge communities are also highly diverse,[56] which may explain the lack of differences in alpha diversity over time and between the reactors as the granules formed. This also supports previous findings of comparable richness between AGS and activated sludge communities.[57]

4.2.2. Mass immigration had limited importance for the AGS community composition. The influent microbial community had lower alpha diversity than the reactor community (Fig. 4A and S5†), which could be explained by the larger variety of microhabitats in the reactor biomass.

The microbial communities in the reactors were highly different in composition from the communities in the influent wastewater (Fig. 4D). This suggests that mass flow immigration was not a key factor in shaping the microbial community in the reactors. Instead, the reactor communities were likely more influenced by environmental and operational factors. In AGS, species sorting, as opposed to immigration, seems to be the main controlling mechanism for the microbial community assembly.[29] This is different to activated sludge, where mass-immigration has been observed to be a major determinant for the assembly of microbial communities.[28] Likely, the biofilm growth mode and long SRT for the large fraction of granules lead to species sorting as the dominant mechanism shaping the microbial community in AGS. The SRT in full-scale AGS varies greatly depending on biomass configuration, ranging from 6.2 ± 2.2 days in the floccular sludge to 142 ± 14.9 days for the large granules (>1.0 mm).[29] Hence, one calculated value of average SRT would not sufficiently describe a full-scale AGS reactor.

4.2.3. The AGS community composition was dynamic over time. The microbial community composition changed over time in both reactors with a higher rate in the early phases, but with continuous changes throughout the study period (Fig. 4B and S6†). Interestingly, the rate of change was similar in R1 and R2, both before and after the reseeding (Fig. S8†), suggesting that the seed of AGS and activated sludge were adapting to the local environment at the same rate. When R1 was reseeded with biomass from R2, the communities of the two reactors converged (Fig. 4B) with only minor dissimilarities among the reactors in the later stages of the study period (Fig. 4D).

The dissimilarity as a function of time gap between samples in R2 (not subjected to reseeding) reached a maximum between samples taken around half a year apart, a local minimum between samples taken one year apart, and thereafter increased at an even longer time gap (Fig. 4C). This indicates seasonal periodicity of the AGS communities, even though a part of the dynamics over time was permanent as the microbial community composition diverged from the seed (Fig. 4B). Seasonal factors at the Österröd AGS plant include temperature, a summer tourist season with increased loads of nutrients, rainy periods with high flows in autumn and winter, and sometimes snowmelt in early spring resulting in higher flows and temperature drops. Nutrient concentrations and temperature have been found to play key roles in the microbial community assembly of AGS,[23,58] and were likely involved in the observed seasonal pattern. Seasonal variability has also been identified as an important factor shaping activated sludge communities.[26,27,59] Seasonal patterns may even affect the flocs and granules in a full-scale AGS plant at varying extent. The lower SRT of flocs than granules possibly make the floccular communities more susceptible to the seasonal variability in environmental factors. Hence, for a comprehensive understanding of the impact of seasonality on the AGS microbial community, granular and floccular biomass would need to be investigated separately over an even longer period.

4.3. Process performance and microbial community dynamics

4.3.1. Suspended solids in the effluent were low. The suspended solid concentration in the effluent from the Österröd AGS reactors was low, on average 10.6 (±5.3) mg L^{-1}. Effluent suspended solids concentrations from full-scale AGS plants range from 5 to 20 mg L^{-1}.[60] Mitigation methods to decrease effluent suspended solids from the AGS process include nitrogen stripping and scum baffles to decrease the rising of lighter biomass.[61] Such measures were implemented at the Österröd AGS plant and likely contributed to the comparably low effluent suspended solids concentrations.

The microbial community in the effluent was different from the reactor biomass, but even more dissimilar to the influent community (Fig. 4D). The suspended solids in the effluent probably originated from the shearing of the outer layers of the granules and flocs to a large extent, resulting in an effluent composition reflecting the surface composition of granules,[52] although growth in suspension likely also contributed to the SS.

4.3.2. Organic matter removal was efficient. The effluent BOD_7 concentrations were low compared to other full-scale AGS plants, on average 6.5 (±2.9) mg L^{-1} (Fig. 7A). For

example, effluent concentrations of BOD_5 were around 10–20 mg L^{-1} at two other AGS plants.[5,8] One possible explanation for the comparably low BOD_7 values here may have been the pre-settling, which was not implemented at the plants in the other studies. The soluble COD was mainly removed at the beginning of the cycle, which supports the findings of abundant PAO- and GAO communities in the reactors, as they are storing carbon anaerobically (the feeding phase of the cycle). Since little soluble COD was removed in the aeration phase, the denitrification was to a large extent dependent on internally stored organic carbon by denitrifying PAOs and GAOs and on endogenous carbon use. The genera of PAOs (*Tetrasphaera*, *Ca.* Accumulibacter and *Dechloromonas*) and GAOs (*Ca.* Competibacter) detected in the reactors indeed contains several clades capable of denitrification.[62–65]

4.3.3. Establishment of nitrogen removal was challenging. Both reactors performed nitrification from the start, which shows that both seeding sludges had active nitrifying communities. Nitrification declined in the period from November 2018 to April/May 2019 (Fig. 7B), which coincides with the disconnection of the CAS and a particularly low abundance of AOB (*Nitrosomonas*) in R1 (Fig. S11†). However, the relative abundances of AOB were low throughout the study period in both reactors. Among NOB, *Ca.* Nitrotoga was mainly detected with smaller populations of *Nitrospira*, declining from November onward (Fig. 5). The detected *Nitrospira* may be complete ammonia oxidisers (Comammox), and hence compete with the AOB.[66] *Ca.* Nitrotoga is well-adapted to low temperatures and has previously been detected in many temperate- and cold-water WWTPs.[67,68] The temperature preferences of *Ca.* Nitrotoga may have contributed to its dynamics over time, with peaks in the winter periods (Fig. 5). The low temperatures, very short cycle times and high nutrient loads (over design capacity) in winter and spring (Fig. 2 and S2†) likely decreased the activity of AOB and NOB and caused elevated effluent ammonium concentrations. Furthermore, the relative abundance of filamentous heterotrophic bacteria (*Ca.* Microthrix and *Trichococcus*) increased in R1 in the winter (Fig. S10†). They probably competed for space and dissolved oxygen with the AOB and NOB, as indicated by the localization of *Trichococcus* at the granule surface, as well as in its interior (Fig. S14C†), and may thereby have contributed to the limited nitrification. When the temperature exceeded 13 °C, from May onward, the cycle times were longer (Fig. 2), and the influent nitrogen concentration increased (Table 1). This provided better conditions for the AOB and NOB, and nitrification increased with effluent concentrations below 5 mg NH_4^+-N per L.

The abundance and activity of nitrifiers were not clearly correlated in the two reactors (data not shown) and abundances were often low (Fig. 5). Efficient nitrification despite low abundances of AOB and NOB has previously been observed in AGS as well as activated sludge.[20,59] Furthermore, actively growing AOB and NOB populations within *Nitrosomonas*, *Ca.* Nitrotoga and *Nitrobacter* have been observed during seasonal nitrification failure, presumably explained by metabolic flexibility.[59]

The reactors performed denitrification with an average nitrate effluent concentration of 8.8 ± 7.6 mg L^{-1} from the AGS plant (Table S3†). Denitrification was suboptimal in the spring of 2019 with a distinct peak in effluent nitrate concentrations from both reactors. From online measurements within a cycle (see Fig. 6 for an example) it was clear that nitrate accumulated as a result of nitrification in the aerated reaction phase. Some nitrate was reduced *via* SND in the aeration phase, possibly by denitrifying PAOs and GAOs using stored organic carbon, since the concentration peak of nitrate was consistently lower than the peak of ammonium. But this assessment is not straightforward. The actual ammonium concentrations may have been underestimated by the online analysers due to ammonium adsorption to the biomass,[69] which would lead an underestimation of the SND. On the other hand, some ammonium was also consumed by assimilation. Within the cycles, complete reduction of nitrate was delayed until the oxygen level dropped, suggesting limited SND. This supports a recent comprehensive modelling study of AGS systems treating municipal wastewater, showing that SND is limited by the anoxic volumes within the granules and the availability of electron donors,[70] probably due to insufficient concentrations of volatile fatty acids (VFA) in the influent. A low concentration of VFA would result in a small penetration depth and thus that only a minor fraction of the microbial community will be exposed, which would limit the denitrification capacity. Higher denitrification rates were furthermore not necessarily correlated with lower effluent concentrations (Fig. S21 and S22†), as high rates often coincided with short cycle times. The effluent concentration of nitrate decreased drastically from August 2019 (Fig. 7D). At that time, the nitrogen load to the AGS decreased due to the commission of the CAS reactor (Fig. S2†), and the cycle times increased (Table 2), resulting in more time for denitrification after the aeration phase. Furthermore, primary sludge hydrolysis started at the WWTP at the end of August 2019 by increasing the sludge level in the primary settlers. This correlated with increased BOD/N-ratio (Table 1) and presumably also increased bioavailability of the organic matter, even though no substantial difference in concentrations of dissolved COD could be detected. Interestingly, the abundance of *Rhodoferax* increased remarkably in both reactors in this period (Fig. S8†), possibly reflecting a preference for easily biodegradable organic matter. *Rhodoferax* has previously been characterised as a core denitrifier in activated sludge capable of acetate utilisation under anoxic conditions.[71]

4.3.4. PAOs were the most abundant guild. The microbial community harboured many PAOs, with *Tetrasphaera* being the most abundant taxa over the entire period (Fig. 5). *Tetrasphaera* has been observed as the principal PAO in several WWTPs treating municipal wastewater.[72] It is fermentative and thereby able to use a broad range of

substrates, besides VFA, and can grow anaerobically.[73] The abundance of *Tetrasphaera* likely reflects the influent composition, where the concentrations of VFA were low (around 20 mg L^{-1}, data not shown). Besides *Tetrasphaera*, PAOs within *Ca.* Accumulibacter and *Dechloromonas* were present in both reactors. GAOs within *Ca.* Competibacter and *Propionivibrio* were also detected in the reactors at varying abundances (Fig. 5). Interestingly, the detected genera of PAOs and GAOs were the same as the ones found at the AGS at Garmerwolde WWTP in the Netherlands[25] indicating high similarity among these guilds across AGS plants.

The fluctuating phosphate concentration in the effluent from both reactors indicated limited phosphorus uptake during the first year (Fig. 7C). This was likely caused by a lack of organic carbon that could diffuse into the granule, where the PAOs were located at all granule depths (Fig. S15†). Online measurements within the AGS cycles showed that the phosphorus uptake rate decreased well before the aeration phase finished, despite considerable phosphorus concentrations in the water (Fig. S16†), which suggests a lack of internally stored organic carbon in the PAOs. GAOs competing for bioavailable carbon during anaerobic feeding could possibly have contributed to the limited phosphate uptake by the PAOs. However, this is questionable given the limited proof of detrimental effects of GAOs on phosphorus removal in full-scale WWTPs.[73] The improved phosphorus removal in both reactors in autumn 2019 (Fig. 7C) could be linked to the increase in BOD/P-ratio and presumable increase of easily bioavailable substrate after the introduction of a hydrolysation in the primary settler. At the same time, the abundance of *Ca.* Accumulibacter (PAO) and *Propionivibrio* (GAO) increased (Fig. 5). In this period, the effluent concentration of phosphate was 0.03 ± 0.01 mg L^{-1} (October 2019, n = 4), which is in the same range as other full-scale AGS plants.[5,8]

4.4. Method considerations

In this study, amplicon sequencing was used as the main method to investigate the microbial community structure over time and between sample types (reactors, influent and effluent). The feasibility of analysing large datasets containing millions of sequences is the main merit of the method as this enables in-depth diversity measurements and thorough statistical analysis.[33] However, all microbial community analysis methods suffer from biases and limitations.[74] Although amplicon sequencing is expected to approximate microbial species composition and relative abundances well,[75] the relative abundance of some taxa was likely underestimated at the expense of others. For example, the abundance of *Ca.* Accumulibacter may be underestimated.[74] However, the distribution patterns of the taxa over time and between sample types, for which amplicon sequencing is widely used in water and wastewater surveys,[76] were likely captured at higher precision.

5. Conclusions

Granulation and community succession were studied in two full-scale aerobic granular sludge reactors for more than 1 year. The microbial community composition was dynamic over time, especially in the first months of the start-up. Seasonal variations in environmental conditions and reactor operation were the main drivers shaping the communities, while the immigration of microorganisms from the influent wastewater had less importance. The key guilds for nutrient removal were similar in composition to those in other full-scale AGS plants with high abundances of PAOs and GAOs.

Seeding sludge and start-up conditions had large influences on the granulation and reactor performance. Non-selective and excessive sludge withdrawal likely hindered the granulation to proceed in R1, and the PAOs and GAOs probably had a positive impact on the granulation in R1 after reseeding of biomass from R2.

The reactor performances were sensitive to short cycle times and high nutrient loads (when the CAS was out of operation), low temperatures, and low BOD/N- and BOD/P-ratios. In this full-scale operation, these factors often coincided, which complicated the cause-and-effect evaluation. Nevertheless, at the end of the study period, the reactors had excellent effluent concentrations of suspended solids, organic matter, nitrogen and phosphorus, when the operational- and environmental conditions were tuned in.

Author contributions

Jennifer Ekholm: conceptualization, methodology, formal analysis, investigation, writing – original draft. Frank Persson: conceptualization, methodology, writing – review & editing, supervision, project administration, funding acquisition. Mark de Blois: conceptualization, methodology, formal analysis, writing – review & editing, supervision, funding acquisition. Oskar Modin: resources, data curation, writing – review & editing. Mario Pronk: writing – review & editing, supervision. Mark C. M. van Loosdrecht: writing – review & editing, supervision. Carolina Suarez: investigation, writing – review & editing. David J. I. Gustavsson: conceptualization, methodology, writing – review & editing, supervision, project administration, funding acquisition. Britt-Marie Wilén: conceptualization, methodology, writing – review & editing, supervision, funding acquisition.

Conflicts of interest

There are no conflicts to declare.

Acknowledgements

We acknowledge the staff at Österröd WWTP for their help and support in sampling, and data collection. Royal HaskoningDHV is acknowledged for their advice and knowledge of the operation of AGS Nereda® systems. This study was funded by the Swedish Water & Wastewater

Association (SVU), Sweden Water Research and the Swedish municipal WWTP operators Uppsala Vatten och Avfall, Gryaab, Käppala Association and Chalmers University of Technology. Members of the project are as well H2OLAND, the municipality of Strömstad, the municipality of Tanum, TU Delft and Royal HaskoningDHV and the municipality of Västervik.

References

1 M. K. de Kreuk, J. J. Heijnen and M. C. M. van Loosdrecht, Simultaneous COD, nitrogen, and phosphate removal by aerobic granular sludge, *Biotechnol. Bioeng.*, 2005, **90**, 761–769.
2 S. Bengtsson, M. de Blois, B.-M. Wilén and D. Gustavsson, A comparison of aerobic granular sludge with conventional and compact biological treatment technologies, *Environ. Technol.*, 2019, **40**, 2769–2778.
3 M. Pronk, A. Giesen, A. Thompson, S. Robertson and M. van Loosdrecht, Aerobic granular biomass technology: advancements in design, applications and further developments, *Water Pract. Technol.*, 2017, **12**, 987–996.
4 P. Kehrein, M. van Loosdrecht, P. Osseweijer and J. Posada, Exploring resource recovery potentials for the aerobic granular sludge process by mass and energy balances–energy, biopolymer and phosphorous recovery from municipal wastewater, *Environ. Sci.: Water Res. Technol.*, 2020, **6**, 2164–2179.
5 M. Pronk, M. K. de Kreuk, B. de Bruin, P. Kamminga, R. Kleerebezem and M. C. M. van Loosdrecht, Full scale performance of the aerobic granular sludge process for sewage treatment, *Water Res.*, 2015, **84**, 207–217.
6 RoyalHaskoningDHV, **https://global.royalhaskoningdhv.com/nereda/projects**, (accessed 2022-01-03).
7 A. Giesen, L. M. M. de Bruin, R. P. Niermans and H. F. van der Roest, Advancements in the application of aerobic granular biomass technology for sustainable treatment of wastewater, *Water Pract. Technol.*, 2013, **8**, 47–54.
8 P. Świątczak and A. Cydzik-Kwiatkowska, Performance and microbial characteristics of biomass in a full-scale aerobic granular sludge wastewater treatment plant, *Environ. Sci. Pollut. Res.*, 2018, **25**, 1655–1669.
9 S. Toja Ortega, M. Pronk and M. K. de Kreuk, Effect of an Increased Particulate COD Load on the Aerobic Granular Sludge Process: A Full Scale Study, *Processes*, 2021, **9**, 1472.
10 G. V. Levin, G. J. Topol and A. G. Tarnay, Operation of full-scale biological phosphorus removal plant, *J. - Water Pollut. Control Fed.*, 1975, **47**, 577–590.
11 E. J. H. van Dijk, V. A. Haaksman, M. C. M. van Loosdrecht and M. Pronk, On the mechanisms for aerobic granulation - model based evaluation, *Water Res.*, 2022, **216**, 118365.
12 M. K. De Kreuk and M. C. M. Van Loosdrecht, Selection of slow growing organisms as a means for improving aerobic granular sludge stability, *Water Sci. Technol.*, 2004, **49**, 7–19.
13 B.-M. Wilén, R. Liébana, F. Persson, O. Modin and M. Hermansson, The mechanisms of granulation of activated sludge in wastewater treatment, its optimization, and impact on effluent quality, *Appl. Microbiol. Biotechnol.*, 2018, **102**, 5005–5020.
14 M. K. Winkler, R. Kleerebezem, M. Strous, K. Chandran and M. C. M. van Loosdrecht, Factors influencing the density of aerobic granular sludge, *Appl. Microbiol. Biotechnol.*, 2013, **97**, 7459–7468.
15 S. J. Sarma, J. H. Tay and A. Chu, Finding knowledge Gaps Aerobic Granulation Technology, *Trends Biotechnol.*, 2017, **35**, 66–78.
16 B. Nguyen Quoc, M. Armenta, J. A. Carter, R. Bucher, P. Sukapanpotharam, S. J. Bryson, D. A. Stahl, H. D. Stensel and M.-K. H. Winkler, An investigation into the optimal granular sludge size for simultaneous nitrogen and phosphate removal, *Water Res.*, 2021, **198**, 117119.
17 J. Xia, L. Ye, H. Ren and X.-X. Zhang, Microbial community structure and function in aerobic granular sludge, *Appl. Microbiol. Biotechnol.*, 2018, **102**, 3967–3979.
18 D. G. Weissbrodt, S. Lochmatter, S. Ebrahimi, P. Rossi, J. Maillard and C. Holliger, Bacterial selection during the formation of early-stage aerobic granules in wastewater treatment systems operated under wash-out dynamics, *Front. Microbiol.*, 2012, **3**, 1–22.
19 A. Gonzalez-Martinez, B. Muñoz-Palazon, A. Rodriguez-Sanchez, P. Maza-Márquez, A. Mikola, J. Gonzalez-Lopez and R. Vahala, Start-up and operation of an aerobic granular sludge system under low working temperature inoculated with cold-adapted activated sludge from Finland, *Bioresour. Technol.*, 2017, **239**, 180–189.
20 E. Szabó, R. Liébana, M. Hermansson, O. Modin, F. Persson and B.-M. Wilén, Microbial Population Dynamics and Ecosystem Functions of Anoxic/Aerobic Granular Sludge in Sequencing Batch Reactors Operated at Different Organic Loading Rates, *Front. Microbiol.*, 2017, **8**, 770.
21 X.-Y. Fan, J.-F. Gao, K.-L. Pan, D.-C. Li, L.-F. Zhang and S.-J. Wang, Shifts in bacterial community composition and abundance of nitrifiers during aerobic granulation in two nitrifying sequencing batch reactors, *Bioresour. Technol.*, 2018, **251**, 99–107.
22 R. Liébana, O. Modin, F. Persson, E. Szabó, M. Hermansson and B.-M. Wilén, Combined Deterministic and Stochastic Processes Control Microbial Succession in Replicate Granular Biofilm Reactors, *Environ. Sci. Technol.*, 2019, **53**(9), 4912–4921.
23 B. Muñoz-Palazon, A. Rodriguez-Sanchez, M. Hurtado-Martinez, J. Gonzalez-Lopez, P. Pfetzing and A. Gonzalez-Martinez, Performance and microbial community structure of aerobic granular bioreactors at different operational temperature, *J. Water Process. Eng.*, 2020, **33**, 101110.
24 M. Layer, A. Adler, E. Reynaert, A. Hernandez, M. Pagni, E. Morgenroth, C. Holliger and N. Derlon, Organic substrate diffusibility governs microbial community composition, nutrient removal performance and kinetics of granulation of aerobic granular sludge, *Water Res.: X*, 2019, **4**, 100033.
25 S. Toja Ortega, M. Pronk and M. K. de Kreuk, Anaerobic hydrolysis of complex substrates in full-scale aerobic

granular sludge: enzymatic activity determined in different sludge fractions, *Appl. Microbiol. Biotechnol.*, 2021, **105**, 6073–6086.

26 J. S. Griffin and G. F. Wells, Regional synchrony in full-scale activated sludge bioreactors due to deterministic microbial community assembly, *ISME J.*, 2017, **11**, 500–511.

27 M. de Celis, I. Belda, R. Ortiz-Álvarez, L. Arregui, D. Marquina, S. Serrano and A. Santos, Tuning up microbiome analysis to monitor WWTPs' biological reactors functioning, *Sci. Rep.*, 2020, **10**, 4079.

28 G. Dottorini, T. Y. Michaelsen, S. Kucheryavskiy, K. S. Andersen, J. M. Kristensen, M. Peces, D. S. Wagner, M. Nierychlo and P. H. Nielsen, Mass-immigration determines the assembly of activated sludge microbial communities, *Proc. Natl. Acad. Sci. U. S. A.*, 2021, **118**, e2021589118.

29 M. Ali, Z. Wang, K. W. Salam, A. R. Hari, M. Pronk, M. C. M. van Loosdrecht and P. E. Saikaly, Importance of Species Sorting and Immigration on the Bacterial Assembly of Different-Sized Aggregates in a Full-Scale Aerobic Granular Sludge Plant, *Environ. Sci. Technol.*, 2019, **53**, 8291–8301.

30 A. Mosquera-Corral, M. De Kreuk, J. Heijnen and M. Van Loosdrecht, Effects of oxygen concentration on N-removal in an aerobic granular sludge reactor, *Water Res.*, 2005, **39**, 2676–2686.

31 APHA, *Standard Methods for the Examination of Water and Wastewater*, American Public Health Association, Washington DC, 2005.

32 J. G. Caporaso, C. L. Lauber, W. A. Walters, D. Berg-Lyons, C. A. Lozupone, P. J. Turnbaugh, N. Fierer, R. Knight and J. I. Gordon, Global patterns of 16S rRNA diversity at a depth of millions of sequences per sample, *Proc. Natl. Acad. Sci. U. S. A.*, 2011, **108**, 4516–4522.

33 L. W. Hugerth, H. A. Wefer, S. Lundin, H. E. Jakobsson, M. Lindberg, S. Rodin, L. Engstrand, A. F. Andersson and F. E. Löffler, DegePrime, a Program for Degenerate Primer Design for Broad-Taxonomic-Range PCR in Microbial Ecology Studies, *Appl. Environ. Microbiol.*, 2014, **80**, 5116–5123.

34 B. J. Callahan, P. J. McMurdie, M. J. Rosen, A. W. Han, A. J. A. Johnson and S. P. Holmes, DADA2: High-resolution sample inference from Illumina amplicon data, *Nat. Methods*, 2016, **13**, 581–583.

35 T. Rognes, T. Flouri, B. Nichols, C. Quince and F. Mahé, VSEARCH: a versatile open source tool for metagenomics, *PeerJ*, 2016, **4**, e2584.

36 O. Modin, R. Liébana, S. Saheb-Alam, B.-M. Wilén, C. Suarez, M. Hermansson and F. Persson, Hill-based dissimilarity indices and null models for analysis of microbial community assembly, *Microbiome*, 2020, **8**, 132.

37 R. C. Edgar, SINTAX: a simple non-Bayesian taxonomy classifier for 16S and ITS sequences, *bioRxiv*, 2016, preprint, p. 074161, DOI: **10.1101/074161**.

38 C. Quast, E. Pruesse, P. Yilmaz, J. Gerken, T. Schweer, P. Yarza, J. Peplies and F. O. Glöckner, The SILVA ribosomal RNA gene database project: improved data processing and web-based tools, *Nucleic Acids Res.*, 2013, **41**, D590–D596.

39 J. Oksanen, F. G. Blanchet, R. Kindt, P. Legendre, P. Minchin, R. B. O'Hara, G. Simpson, P. Solymos, M. H. H. Stevens and H. Wagner, Vegan: Community Ecology Package, *R Package Version. 2.0-10*, CRAN, 2013.

40 P. J. McMurdie and S. Holmes, phyloseq: An R Package for Reproducible Interactive Analysis and Graphics of Microbiome Census Data, *PLoS One*, 2013, **8**, e61217.

41 M. Kawaharasaki, H. Tanaka, T. Kanagawa and K. Nakamura, In situ identification of polyphosphate-accumulating bacteria in activated sludge by dual staining with rRNA-targeted oligonucleotide probes and 4′,6-diamidino-2-phenylindol (DAPI) at a polyphosphate-probing concentration, *Water Res.*, 1999, **33**, 257–265.

42 J. Schindelin, I. Arganda-Carreras, E. Frise, V. Kaynig, M. Longair, T. Pietzsch, S. Preibisch, C. Rueden, S. Saalfeld, B. Schmid, J.-Y. Tinevez, D. J. White, V. Hartenstein, K. Eliceiri, P. Tomancak and A. Cardona, Fiji: an open-source platform for biological-image analysis, *Nat. Methods*, 2012, **9**, 676–682.

43 S. Preibisch, S. Saalfeld and P. Tomancak, Globally optimal stitching of tiled 3D microscopic image acquisitions, *Bioinformatics*, 2009, **25**, 1463–1465.

44 L. Jost, Entropy and diversity, *Oikos*, 2006, **113**, 363–375.

45 A. Chao, C.-H. Chiu and L. Jost, Unifying Species Diversity, Phylogenetic Diversity, Functional Diversity, and Related Similarity and Differentiation Measures Through Hill Numbers, *Annu. Rev. Ecol. Evol. Syst.*, 2014, **45**, 297–324.

46 S. Bengtsson, M. de Blois, B.-M. Wilén and D. Gustavsson, Treatment of municipal wastewater with aerobic granular sludge, *Crit. Rev. Environ. Sci. Technol.*, 2018, **48**, 119–166.

47 R. Hamza, A. Rabii, F.-z. Ezzahraoui, G. Morgan and O. T. Iorhemen, A review of the state of development of aerobic granular sludge technology over the last 20 years: Full-scale applications and resource recovery, *Case Stud. Chem. Environ. Eng.*, 2022, **5**, 100173.

48 S. L. D. S. Rollemberg, A. R. M. Barros, J. P. M. de Lima, A. F. Santos, P. I. M. Firmino and A. B. dos Santos, Influence of sequencing batch reactor configuration on aerobic granules growth: Engineering and microbiological aspects, *J. Cleaner Prod.*, 2019, **238**, 117906.

49 B.-J. Ni, W.-M. Xie, S.-G. Liu, H.-Q. Yu, Y.-Z. Wang, G. Wang and X.-L. Dai, Granulation of activated sludge in a pilot-scale sequencing batch reactor for the treatment of low-strength municipal wastewater, *Water Res.*, 2009, **43**, 751–761.

50 A. Gonzalez-Martinez, B. Muñoz-Palazon, P. Maza-Márquez, A. Rodriguez-Sanchez, J. Gonzalez-Lopez and R. Vahala, Performance and microbial community structure of a polar Arctic Circle aerobic granular sludge system operating at low temperature, *Bioresour. Technol.*, 2018, **256**, 22–29.

51 J. Wagner, D. G. Weissbrodt, V. Manguin, R. H. Ribeiro da Costa, E. Morgenroth and N. Derlon, Effect of particulate organic substrate on aerobic granulation and operating conditions of sequencing batch reactors, *Water Res.*, 2015, **85**, 158–166.

52 E. Szabó, R. Liébana, M. Hermansson, O. Modin, F. Persson and B.-M. Wilén, Comparison of the bacterial community

composition in the granular and the suspended phase of sequencing batch reactors, *AMB Express*, 2017, **7**, 168.

53 M. Layer, A. Brison, M. G. Villodres, M. Stähle, F. Házi, I. Takács, E. Morgenroth and N. Derlon, Microbial conversion pathways of particulate organic substrate conversion in aerobic granular sludge systems: limited anaerobic conversion and the essential role of flocs, *Environ. Sci.: Water Res. Technol.*, 2022, **8**, 1236–1251.

54 M. K. D. Dueholm, M. Nierychlo, K. S. Andersen, V. Rudkjøbing, S. Knutsson, M. Albertsen and P. H. Nielsen, MiDAS 4: A global catalogue of full-length 16S rRNA gene sequences and taxonomy for studies of bacterial communities in wastewater treatment plants, *Nat. Commun.*, 2022, **13**, 1–15.

55 H.-C. Flemming, J. Wingender, U. Szewzyk, P. Steinberg, S. A. Rice and S. Kjelleberg, Biofilms: an emergent form of bacterial life, *Nat. Rev. Microbiol.*, 2016, **14**, 563–575.

56 L. Wu, D. Ning, B. Zhang, Y. Li, P. Zhang, X. Shan, Q. Zhang, M. R. Brown, Z. Li, J. D. Van Nostrand, F. Ling, N. Xiao, Y. Zhang, J. Vierheilig, G. F. Wells, Y. Yang, Y. Deng, Q. Tu, A. Wang, D. Acevedo, M. Agullo-Barcelo, P. J. J. Alvarez, L. Alvarez-Cohen, G. L. Andersen, J. C. de Araujo, K. F. Boehnke, P. Bond, C. B. Bott, P. Bovio, R. K. Brewster, F. Bux, A. Cabezas, L. Cabrol, S. Chen, C. S. Criddle, Y. Deng, C. Etchebehere, A. Ford, D. Frigon, J. Sanabria, J. S. Griffin, A. Z. Gu, M. Habagil, L. Hale, S. D. Hardeman, M. Harmon, H. Horn, Z. Hu, S. Jauffur, D. R. Johnson, J. Keller, A. Keucken, S. Kumari, C. D. Leal, L. A. Lebrun, J. Lee, M. Lee, Z. M. P. Lee, Y. Li, Z. Li, M. Li, X. Li, F. Ling, Y. Liu, R. G. Luthy, L. C. Mendonça-Hagler, F. G. R. de Menezes, A. J. Meyers, A. Mohebbi, P. H. Nielsen, D. Ning, A. Oehmen, A. Palmer, P. Parameswaran, J. Park, D. Patsch, V. Reginatto, F. L. de los Reyes, B. E. Rittmann, A. Noyola, S. Rossetti, X. Shan, J. Sidhu, W. T. Sloan, K. Smith, O. V. de Sousa, D. A. Stahl, K. Stephens, R. Tian, J. M. Tiedje, N. B. Tooker, Q. Tu, J. D. Van Nostrand, D. De los Cobos Vasconcelos, J. Vierheilig, M. Wagner, S. Wakelin, A. Wang, B. Wang, J. E. Weaver, G. F. Wells, S. West, P. Wilmes, S.-G. Woo, L. Wu, J.-H. Wu, L. Wu, C. Xi, N. Xiao, M. Xu, T. Yan, Y. Yang, M. Yang, M. Young, H. Yue, B. Zhang, P. Zhang, Q. Zhang, Y. Zhang, T. Zhang, Q. Zhang, W. Zhang, Y. Zhang, H. Zhou, J. Zhou, X. Wen, T. P. Curtis, Q. He, Z. He, M. R. Brown, T. Zhang, Z. He, J. Keller, P. H. Nielsen, P. J. J. Alvarez, C. S. Criddle, M. Wagner, J. M. Tiedje, Q. He, T. P. Curtis, D. A. Stahl, L. Alvarez-Cohen, B. E. Rittmann, X. Wen, J. Zhou and C. Global Water Microbiome, Global diversity and biogeography of bacterial communities in wastewater treatment plants, *Nat. Microbiol.*, 2019, **4**, 1183–1195.

57 M. K. H. Winkler, R. Kleerebezem, M. Strous, K. Chandran and M. C. M. Van Loosdrecht, Factors influencing the density of aerobic granular sludge, *Appl. Microbiol. Biotechnol.*, 2013, **97**, 7459–7468.

58 P. Xu, Z. Xie, L. Shi, X. Yan, Z. Fu, J. Ma, W. Zhang, H. Wang, B. Xu and Q. He, Distinct responses of aerobic granular sludge sequencing batch reactors to nitrogen and phosphorus deficient conditions, *Sci. Total Environ.*, 2022, **834**, 155369.

59 J. Johnston, S. Behrens and S.-J. Liu, Seasonal Dynamics of the Activated Sludge Microbiome in Sequencing Batch Reactors, Assessed Using 16S rRNA Transcript Amplicon Sequencing, *Appl. Environ. Microbiol.*, 2020, **86**, e00597-060520.

60 M. Pronk, B. Abbas, S. H. K. Al-zuhairy, R. Kraan, R. Kleerebezem and M. C. M. van Loosdrecht, Effect and behaviour of different substrates in relation to the formation of aerobic granular sludge, *Appl. Microbiol. Biotechnol.*, 2015, **99**, 5257–5268.

61 E. J. H. van Dijk, M. Pronk and M. C. M. van Loosdrecht, Controlling effluent suspended solids in the aerobic granular sludge process, *Water Res.*, 2018, **147**, 50–59.

62 H. Gao, Y. Mao, X. Zhao, W.-T. Liu, T. Zhang and G. Wells, Genome-centric metagenomics resolves microbial diversity and prevalent truncated denitrification pathways in a denitrifying PAO-enriched bioprocess, *Water Res.*, 2019, **155**, 275–287.

63 R. Marques, A. Ribera-Guardia, J. Santos, G. Carvalho, M. A. M. Reis, M. Pijuan and A. Oehmen, Denitrifying capabilities of Tetrasphaera and their contribution towards nitrous oxide production in enhanced biological phosphorus removal processes, *Water Res.*, 2018, **137**, 262–272.

64 F. Petriglieri, C. Singleton, M. Peces, J. F. Petersen, M. Nierychlo and P. H. Nielsen, "Candidatus Dechloromonas phosphoritropha" and "Ca. D. phosphorivorans", novel polyphosphate accumulating organisms abundant in wastewater treatment systems, *ISME J.*, 2021, **15**, 3605–3614.

65 Y. Wang, H. Gao and G. F. Wells, Integrated omics analyses reveal differential gene expression and potential for cooperation between denitrifying polyphosphate and glycogen accumulating organisms, *Environ. Microbiol.*, 2021, **23**, 3274–3293.

66 H. Daims, S. Lücker and M. Wagner, A new perspective on microbes formerly known as nitrite-oxidizing bacteria, *Trends Microbiol.*, 2016, **24**, 699–712.

67 S. Lücker, J. Schwarz, C. Gruber-Dorninger, E. Spieck, M. Wagner and H. Daims, *Nitrotoga*-like bacteria are previously unrecognized key nitrite oxidizers in full-scale wastewater treatment plants, *ISME J.*, 2015, **9**, 708–720.

68 E. Spieck, S. Wegen and S. Keuter, Relevance of *Candidatus* Nitrotoga for nitrite oxidation in technical nitrogen removal systems, *Appl. Microbiol. Biotechnol.*, 2021, **105**, 7123–7139.

69 J. Bassin, M. Pronk, R. Kraan, R. Kleerebezem and M. Van Loosdrecht, Ammonium adsorption in aerobic granular sludge, activated sludge and anammox granules, *Water Res.*, 2011, **45**, 5257–5265.

70 M. Layer, M. G. Villodres, A. Hernandez, E. Reynaert, E. Morgenroth and N. Derlon, Limited simultaneous nitrification-denitrification (SND) in aerobic granular sludge systems treating municipal wastewater: Mechanisms and practical implications, *Water Res.: X*, 2020, **7**, 100048.

71 S. J. McIlroy, A. Starnawska, P. Starnawski, A. M. Saunders, M. Nierychlo, P. H. Nielsen and J. L. Nielsen, Identification

of active denitrifiers in full-scale nutrient removal wastewater treatment systems, *Environ. Microbiol.*, 2016, **18**, 50–64.

72 M. Stokholm-Bjerregaard, S. J. McIlroy, M. Nierychlo, S. M. Karst, M. Albertsen and P. H. Nielsen, A Critical Assessment of the Microorganisms Proposed to be Important to Enhanced Biological Phosphorus Removal in Full-Scale Wastewater Treatment Systems, *Front. Microbiol.*, 2017, **8**, 718.

73 P. H. Nielsen, S. J. McIlroy, M. Albertsen and M. Nierychlo, Re-evaluating the microbiology of the enhanced biological phosphorus removal process, *Curr. Opin. Biotechnol.*, 2019, **57**, 111–118.

74 H. B. C. Kleikamp, D. Grouzdev, P. Schaasberg, R. van Valderen, R. van der Zwaan, R. van de Wijgaart, Y. Lin, B. Abbas, M. Pronk, M. C. M. van Loosdrecht and M. Pabst, Comparative metaproteomics demonstrates different views on the complex granular sludge microbiome, *bioRxiv*, 2022, DOI: **10.1101/2022.03.07.483319**.

75 B. Tan, C. Ng, J. Nshimyimana, L.-L. Loh, K. Gin and J. Thompson, Next-generation sequencing (NGS) for assessment of microbial water quality: current progress, challenges, and future opportunities, *Front. Microbiol.*, 2015, **6**, 1027.

76 E. Garner, B. C. Davis, E. Milligan, M. F. Blair, I. Keenum, A. Maile-Moskowitz, J. Pan, M. Gnegy, K. Liguori, S. Gupta, A. J. Prussin, L. C. Marr, L. S. Heath, P. J. Vikesland, L. Zhang and A. Pruden, Next generation sequencing approaches to evaluate water and wastewater quality, *Water Res.*, 2021, **194**, 116907.

